New Leading Contribution to Neutrinoless Double-β Decay

Vincenzo Cirigliano,[1] Wouter Dekens,[1] Jordy de Vries,[2] Michael L. Graesser,[1]
Emanuele Mereghetti,[1] Saori Pastore,[1] and Ubirajara van Kolck[3,4]

[1]*Theoretical Division, Los Alamos National Laboratory, Los Alamos, New Mexico 87545, USA*
[2]*Nikhef, Theory Group, Science Park 105, 1098 XG Amsterdam, The Netherlands*
[3]*Institut de Physique Nucléaire, CNRS/IN2P3, Université Paris-Sud, Université Paris-Saclay, 91406 Orsay, France*
[4]*Department of Physics, University of Arizona, Tucson, Arizona 85721, USA*

Within the framework of chiral effective field theory, we discuss the leading contributions to the neutrinoless double-beta decay transition operator induced by light Majorana neutrinos. Based on renormalization arguments in both dimensional regularization with minimal subtraction and a coordinate-space cutoff scheme, we show the need to introduce a leading-order short-range operator, missing in all current calculations. We discuss strategies to determine the finite part of the short-range coupling by matching to lattice QCD or by relating it via chiral symmetry to isospin-breaking observables in the two-nucleon sector. Finally, we speculate on the impact of this new contribution on nuclear matrix elements of relevance to experiment.

Introduction.—Neutrinoless double-beta decay ($0\nu\beta\beta$) is the most sensitive laboratory probe of lepton number violation (LNV). In $0\nu\beta\beta$, L is violated by two units when two neutrons in a nucleus turn into two protons, with the emission of two electrons and no neutrinos. The observation of $0\nu\beta\beta$ would demonstrate that neutrinos are Majorana fermions [1], shed light on the mechanism of neutrino mass generation [2–4], and give insight into leptogenesis scenarios for the generation of the matter-antimatter asymmetry in the Universe [5].

$0\nu\beta\beta$ is actively being searched for in a number of even-even nuclei for which single-β decay is energetically forbidden. Current experimental limits [6–15] on the half-lives are at the level of $T_{1/2} > 5.3 \times 10^{25}$ y for ^{76}Ge [12] and $T_{1/2} > 1.07 \times 10^{26}$ y for ^{136}Xe [10], with next-generation ton-scale experiments aiming at improvements in sensitivity by two orders of magnitude.

$0\nu\beta\beta$ can be generated by a variety of dynamical LNV mechanisms, which, in an effective field theory (EFT) approach to new physics, are parametrized by $\Delta L = 2$ operators of odd dimension greater than 4 [16–22]. If the mass scale associated with LNV is much higher than the electroweak scale, the only low-energy manifestation of this new physics is a Majorana mass for light neutrinos, encoded in a single gauge-invariant dimension-five

operator [16], which induces $0\nu\beta\beta$ through light Majorana-neutrino exchange [23,24]. To interpret positive or null $0\nu\beta\beta$ results in this minimal scenario, it is crucial to have good control over the relevant hadronic and nuclear matrix elements. Current knowledge of these is not satisfactory [25], as various many-body approaches lead to estimates that differ by a factor of 2–3 and most calculations are not based on a modern EFT analysis. In Ref. [26], a first step was presented towards the analysis of $0\nu\beta\beta$ induced by a light Majorana neutrino in the chiral EFT framework [27–29], which provides a systematic expansion of hadronic amplitudes in p/Λ_χ, where $p \sim m_\pi \sim k_F \sim \mathcal{O}(100\,\text{MeV})$ and $\Lambda_\chi \sim 4\pi F_\pi \sim m_N \sim \mathcal{O}(1\,\text{GeV})$. The $0\nu\beta\beta$ transition operators were derived up to next-to-next-to-leading order (N^{2}LO) in Weinberg's power-counting scheme [30,31].

In this Letter, we demonstrate that Weinberg's scheme for $0\nu\beta\beta$ assumed in Ref. [26] breaks down and any consistent power counting requires a leading-order (LO) short-range $\Delta L = 2$ operator, whose effect is missing in all current calculations. Our argument is based on renormalization. Using two different schemes (dimensional regularization with minimal subtraction and a coordinate-space cutoff), we show that, once the strong nucleon-nucleon scattering amplitude is made finite and independent of the ultraviolet regulator, an additional $\Delta L = 2$ contact operator with coupling g_ν^{NN} has to be introduced to make the $nn \to ppee$ amplitude finite and regulator independent. The finite part of g_ν^{NN}, which encodes hard-neutrino exchange, can be determined by (i) matching the chiral EFT $nn \to ppee$ amplitude to future lattice QCD

calculations and (ii) relating it via chiral symmetry to electromagnetic low-energy constants (LECs) that control isospin breaking in the two-nucleon sector. A combination of couplings involving g_ν^{NN} can be fit to nucleon-nucleon charge-independence-breaking (CIB) observables, confirming the LO scaling of this coupling. Based on this, we argue that the impact of g_ν^{NN} on nuclear matrix elements of relevance to experiments can be significant, which has consequences for the interpretation of $0\nu\beta\beta$ experiments in terms of the light Majorana-neutrino mass.

The need for a LO short-range $\Delta L = 2$ interaction.—We consider a scenario in which LNV at low energy is dominated by the electron-neutrino Majorana mass

$$\mathcal{L}_{\Delta L=2} = -\frac{m_{\beta\beta}}{2} \nu_{eL}^T C \nu_{eL}, \qquad (1)$$

where $C = i\gamma_2\gamma_0$ denotes the charge conjugation matrix.

The nuclear effective Hamiltonian can be written as

$$H_{\text{eff}} = H_{\text{strong}} + 2G_F^2 V_{ud}^2 m_{\beta\beta}\bar{e}_L C \bar{e}_L^T V_\nu, \qquad (2)$$

in terms of the Fermi constant G_F and the V_{ud} element of the Cabibbo-Kobayashi-Maskawa matrix [32,33]. The neutrino potential V_ν can be obtained from two-nucleon irreducible diagrams mediating $nn \to ppee$ to a given order in p/Λ_χ. Within Weinberg's power counting, the only LO contribution [26] comes from the exchange of potential neutrinos, with $q^0 \ll |\mathbf{q}|$,

$$V_{\nu,0}(\mathbf{q}) = \tau^{(1)+}\tau^{(2)+}\frac{1}{\mathbf{q}^2}\left(1 - g_A^2\boldsymbol{\sigma}^{(1)}\cdot\boldsymbol{\sigma}^{(2)}\right.$$
$$\left. + g_A^2\boldsymbol{\sigma}^{(1)}\cdot\mathbf{q}\,\boldsymbol{\sigma}^{(2)}\cdot\mathbf{q}\frac{2m_\pi^2 + \mathbf{q}^2}{(\mathbf{q}^2 + m_\pi^2)^2}\right), \qquad (3)$$

where $g_A \simeq 1.27$ is the nucleon axial coupling, m_π is the pion mass, and $\mathbf{q}$ is the momentum transfer. N^2LO terms arise from corrections to the single nucleon weak currents, irreducible one-loop diagrams, and contact interactions mediating $\pi\pi \to ee$, $n \to p\pi^+ee$, and $nn \to ppee$. In particular, the short-range potential includes a two-nucleon term [26]

$$V_{\nu,CT} = -2g_\nu^{NN}\tau^{(1)+}\tau^{(2)+}, \qquad (4)$$

where the LEC g_ν^{NN} is $\mathcal{O}((4\pi F_\pi)^{-2})$ in Weinberg's counting and $F_\pi = 92.2$ MeV is the pion decay constant. However, it is known that Weinberg's power counting leads to inconsistent results in nucleon-nucleon scattering [34–37] and nuclear processes mediated by external currents [38], due to a conflict between naive dimensional analysis and nonperturbative renormalization. We therefore investigate the scaling of g_ν^{NN} by studying the amplitude $\mathcal{A}(nn \to ppee) \equiv \mathcal{A}_{\Delta L=2}$ with strong interactions H_{strong} included nonperturbatively.

We work at LO in chiral EFT and focus on the scattering of two neutrons to two protons in the $^1S_0$ wave, where H_{strong} has short-range and Yukawa components,

$$V_0(\mathbf{q}) = \tilde{C} + V_\pi(\mathbf{q}), \qquad V_\pi(\mathbf{q}) = -\frac{g_A^2}{4F_\pi^2}\frac{m_\pi^2}{\mathbf{q}^2 + m_\pi^2}, \qquad (5)$$

with $\tilde{C} \sim \mathcal{O}(F_\pi^{-2}, m_\pi^2 F_\pi^{-4})$ [31,34,35]. We have checked that transitions involving higher partial waves such as $^3P_{0,1} \to {}^3P_{0,1}$ are correctly renormalized and do not require enhanced $\Delta L = 2$ counterterms.

The contributions to $\mathcal{A}_{\Delta L=2}$ from the exchange of a light neutrino ($\mathcal{A}_{\Delta L=2}^{(\nu)}$) are shown in Fig. 1. The blue ellipse denotes the iteration of the Yukawa potential $V_\pi(\mathbf{q})$. The diagrams in the second and third rows include an infinite number of bubbles, dressed with iterations of V_π. Without loss of generality for our arguments, we use the kinematics $n(\mathbf{p})n(-\mathbf{p}) \to p(\mathbf{p}')p(-\mathbf{p}')e(\mathbf{p}_{e1}=0)e(\mathbf{p}_{e2}=0)$, with $|\mathbf{p}| = 1$ MeV and, correspondingly, $|\mathbf{p}'| = 38$ MeV.

$\mathcal{A}_{\Delta L=2}^{(\nu)}$ can be expressed in terms of the Yukawa "in" and "out" wave functions $\chi_\mathbf{p}^\pm(\mathbf{r})$ and the propagators $G_E^\pm(\mathbf{r},\mathbf{r}') = \langle\mathbf{r}'|(E-T-V_\pi\pm i0^+)^{-1}|\mathbf{r}\rangle$ [34,37]. Observing that the bubble diagrams in Fig. 1 are related to $G_E^+(\mathbf{0},\mathbf{0})$, while the triangles dressed by Yukawa potentials are related to $\chi_\mathbf{p}^+(\mathbf{0})$ and $\chi_{\mathbf{p}'}^-(\mathbf{0})^* = \chi_{\mathbf{p}'}^+(\mathbf{0})$ [34], the LO amplitude reads

$$\mathcal{A}_{\Delta L=2}^{(\nu)} = \mathcal{A}_A + K_{E'}\mathcal{A}_B + \overline{\mathcal{A}_B}K_E + K_{E'}\mathcal{A}_C K_E,$$
$$K_E = \frac{\chi_\mathbf{p}^+(\mathbf{0})\tilde{C}}{1 - \tilde{C}G_E^+(\mathbf{0},\mathbf{0})}, \qquad (6)$$

where $\mathcal{A}_A$, $\mathcal{A}_B$, and $\mathcal{A}_C$ denote the first diagram in the first, second, and third rows of Fig. 1, respectively (without the wave functions at 0, in the case of $\mathcal{A}_B$ and $\mathcal{A}_C$). $\overline{\mathcal{A}_B}$ is similar to $\mathcal{A}_B$ and is not shown in Fig. 1.
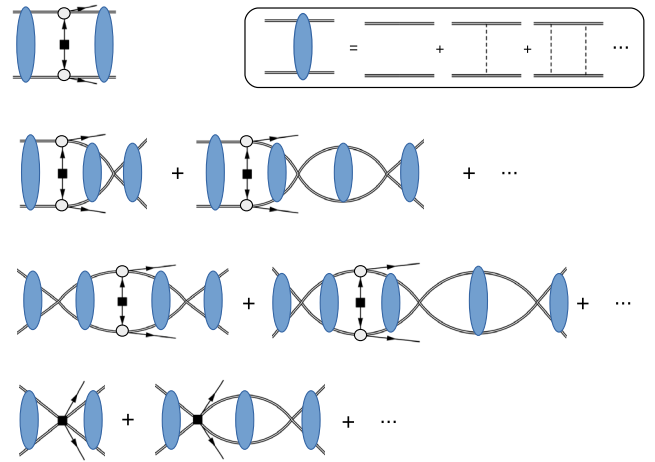

FIG. 1. Diagrammatic representation of LO contributions to $nn \to ppee$. Double, dashed, and plain lines denote nucleons, pions, and leptons, respectively. Gray circles denote the nucleon axial and vector currents, and the black square denotes an insertion of $m_{\beta\beta}$. The blue ellipse represents iteration of V_π. In the counterterm amplitude (fourth line) the black square represents g_ν^{NN}. The ellipses in the second to fourth lines denote diagrams with arbitrary numbers of bubble insertions.

To study the renormalization of the $\Delta L = 2$ amplitude, we now discuss the divergence structure of $\mathcal{A}^{(\nu)}_{\Delta L=2}$. $\chi^+_{\mathbf{p}}(\mathbf{0})$ is finite and the divergence in $G^+_E(\mathbf{0},\mathbf{0})$ is absorbed by $\tilde{C}^{-1}$, so that K_E is finite and scheme independent [34]. We note that (i) all diagrams in $\mathcal{A}_A$ are finite. The tree level is finite and each V_π iteration improves the convergence by bringing in a factor of $d^3\mathbf{k}/(\mathbf{k}^2)^2$, where one $\mathbf{k}^2$ comes from the pion propagator and the other from the two-nucleon propagator. (ii) All the diagrams in $\mathcal{A}_B$ and $\bar{\mathcal{A}}_B$ are finite. The first loop goes as $d^3\mathbf{k}/(\mathbf{k}^2)^2$, while V_π insertions further improve the convergence. (iii) The first two-loop diagram in $\mathcal{A}_C$ has a logarithmic divergence, which stems from an insertion of the most singular component of the neutrino potential, namely,

$$\tilde{V}_\nu(\mathbf{q}) = \tau^{(1)+}\tau^{(2)+}\frac{1}{\mathbf{q}^2}\left(1 - \frac{2}{3}g_A^2\boldsymbol{\sigma}^{(1)}\cdot\boldsymbol{\sigma}^{(2)}\right). \quad (7)$$

The two-loop diagram with insertion of $V_{\nu,0} - \tilde{V}_\nu$ and higher-loop diagrams are convergent.

We focus on $\mathcal{A}_C$ and write $\mathcal{A}_C = \mathcal{A}^{(\mathrm{div})}_C + \delta\mathcal{A}_C$. In dimensional regularization,

$$\mathcal{A}^{(\mathrm{div})}_C = -\left(\frac{m_N}{4\pi}\right)^2(1+2g_A^2)[\Delta + L_{\mathbf{p},\mathbf{p}'}(\mu)],$$

$$L_{\mathbf{p},\mathbf{p}'}(\mu) = \frac{1}{2}\left(\log\frac{\mu^2}{-(|\mathbf{p}|+|\mathbf{p}'|)^2+i0^+} + 1\right), \quad (8)$$

where $\Delta \equiv [1/(4-d) - \gamma + \log 4\pi]/2$. The divergence for $d \to 4$ can be removed by introducing g^{NN}_ν at LO. The counterterm amplitude, shown in the fourth line of Fig. 1, reads

$$\mathcal{A}^{(NN)}_{\Delta L=2} = K_{E'}\frac{2g^{NN}_\nu}{\tilde{C}^2}K_E, \quad (9)$$

and we can renormalize $\mathcal{A}_{\Delta L=2}$ by replacing $\mathcal{A}_C \to \mathcal{A}_C + 2g^{NN}_\nu/\tilde{C}^2$ in Eq. (6). In the $\overline{\mathrm{MS}}$ scheme,

$$\mathcal{A}_C \to \delta\mathcal{A}_C + \left(\frac{m_N}{4\pi}\right)^2\left[2\tilde{g}^{NN}_\nu(\mu) - (1+2g_A^2)L_{\mathbf{p},\mathbf{p}'}(\mu)\right] \quad (10)$$

after defining the dimensionless coupling

$$\tilde{g}^{NN}_\nu = \left(\frac{4\pi}{m_N\tilde{C}}\right)^2 g^{NN}_\nu. \quad (11)$$

This coupling obeys the renormalization-group equation (RGE)

$$\mu\frac{d\tilde{g}^{NN}_\nu}{d\mu} = \frac{1}{2}(1+2g_A^2), \quad (12)$$

confirming that $\tilde{g}^{NN}_\nu \sim \mathcal{O}(1)$. Since $\tilde{C}(\mu = m_\pi) \approx -0.9/F_\pi^2$, we find that $g^{NN}_\nu \sim \mathcal{O}(F_\pi^{-2})$ instead of $\mathcal{O}((4\pi F_\pi)^{-2})$. A similar enhancement also occurs in four-nucleon couplings induced by higher-dimensional LNV operators. Treating V_π

as a subleading correction [35,39] is equivalent to working to LO in pionless EFT and does not affect our conclusions about the importance of g^{NN}_ν [26]. Details on how to obtain $\delta\mathcal{A}_C$ will be provided in future work [40].

$\mathcal{A}_{\Delta L=2}$ *in a cutoff scheme.*—The need for a LO counterterm can be demonstrated also in a coordinate-space scheme that makes no direct reference to Feynman diagrams. In this approach, we regulate the short-range part of V_0 with a smeared δ function,

$$\tilde{C}\delta^{(3)}(\mathbf{r}) \to \frac{\tilde{C}(R_S)}{(\sqrt{\pi}R_S)^3}\exp\left(-\frac{r^2}{R_S^2}\right) \equiv \tilde{C}(R_S)\delta^{(3)}_{R_S}(\mathbf{r}), \quad (13)$$

and obtain $\psi^-_{\mathbf{p}'}(\mathbf{r})$ and $\psi^+_{\mathbf{p}}(\mathbf{r})$ by solving the Schrödinger equation. We determine $\tilde{C}(R_S)$ by requiring that the $^1S_0$ scattering length be reproduced ($\tilde{C} \approx -0.4/F_\pi^2$ at $R_S = 0.8$ fm). We find that $1/\tilde{C}(R_S)$ has linear $(1/R_S)$ and logarithmic divergences [35] and that the $^1S_0$ phase shifts at nonzero momentum are indeed R_S independent.

We then compute

$$\mathcal{A}^{(\nu)}_{\Delta L=2} = -\int d^3\mathbf{r}\,\psi^-_{\mathbf{p}'}(\mathbf{r})^* V_{\nu,0}(\mathbf{r})\psi^+_{\mathbf{p}}(\mathbf{r}), \quad (14)$$

where $V_{\nu,0}(\mathbf{r})$ is obtained by Fourier transforming the $^1S_0$ projection of Eq. (3). In Fig. 2, we plot $\mathcal{A}^{(\nu)}_{\Delta L=2}$ as a function of R_S. The plot displays a logarithmic dependence on R_S [analogous to the $\log\mu$ dependence in Eq. (10)] as well as milder powerlike behavior. Therefore, to obtain a physical, regulator-independent amplitude one needs to include a LO counterterm, given in r space by $V_{\nu,CT}(\mathbf{r}) = -2g^{NN}_\nu(R_S)\delta^{(3)}_{R_S}(\mathbf{r})$. The corresponding amplitude,
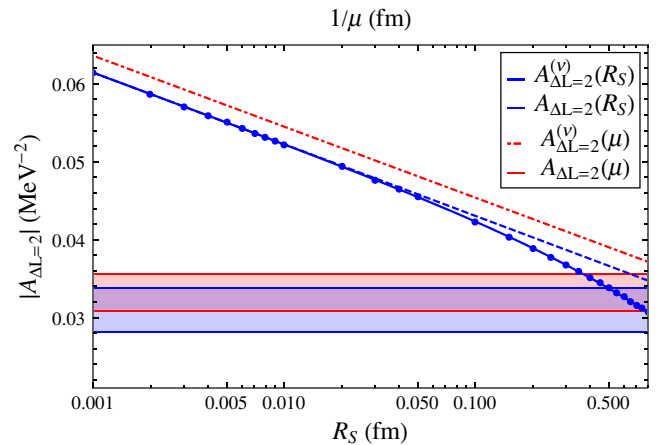

FIG. 2. Matrix element $\mathcal{A}^{(\nu)}_{\Delta L=2}$ for $|\mathbf{p}| = 1$ MeV and $|\mathbf{p}'| = 38$ MeV, as a function of R_S. The dashed line shows a fit to $a + b\log R_S$, which captures the small R_S behavior. The solid line corresponds to a fit that includes $\mathcal{O}(R_S, R_S\log R_S)$ power corrections. The dash-dotted line shows $\mathcal{A}^{(\nu)}_{\Delta L=2}$ in $\overline{\mathrm{MS}}$ as a function of $1/\mu$. The horizontal bands represent the total amplitude $\mathcal{A}_{\Delta L=2}$ with $g^{NN}_\nu = (C_1 + C_2)/2$, as discussed in the main text.

$$\mathcal{A}^{(\mathrm{NN})}_{\Delta L=2} = - \int d^3\mathbf{r}\, \psi^-_{\mathbf{p}'}(\mathbf{r})^* V_{\nu,CT}(\mathbf{r}) \psi^+_{\mathbf{p}}(\mathbf{r}), \qquad (15)$$

is also regulator dependent. As expected from Eq. (9), we find its leading divergent behavior to be well reproduced by $1/\tilde{C}(R_S)^2$. We can then make $\mathcal{A}_{\Delta L=2} = \mathcal{A}^{(\nu)}_{\Delta L=2} + \mathcal{A}^{(\mathrm{NN})}_{\Delta L=2}$ finite for $R_S \to 0$ and R_S independent by choosing $\tilde{g}^{\mathrm{NN}}_\nu(R_S) = -(a/2)(1+2g^2_A)\log R_S + b + c R_S + \cdots$, with the coefficient of the logarithm quite close to the $\overline{\mathrm{MS}}$ expectation $a = 1$.

Relating g^{NN}_ν to electromagnetic isospin violation.—The finite part of g^{NN}_ν can be obtained by matching the chiral EFT amplitude to a lattice QCD calculation performed at the same kinematic point, as it is done in the strong-interacting sector [41]. First lattice results related to double-beta decay are starting to appear [42,43].

We now discuss a complementary estimate based on the fact that the short-range operators and associated LECs arising in $0\nu\beta\beta$ and electromagnetic processes are closely related [26]. In the electromagnetic case, the short-range hadronic operators arise from amplitudes in the underlying theory involving two insertions of the electromagnetic current with exchange of hard virtual photons [44,45]. In the $\Delta L = 2$ case, up to a proportionality factor, the *same* operators are generated by the insertion of two weak currents with exchange of hard neutrinos. This comes about because the neutrino propagator and weak vertices combine to give a massless gauge-boson propagator in Feynman gauge, multiplied by $8G^2_F V^2_{ud} m_{\beta\beta} \bar{e}_L e^c_L$ [26]. The LECs needed for $0\nu\beta\beta$ are therefore related to the LECs associated with the isospin $I = 2$ component of the product of two electromagnetic currents, which belongs to the $5_L \times 1_R$ irreducible representation of chiral $\mathrm{SU}(2)_L \times \mathrm{SU}(2)_R$.

Only two independent four-nucleon operators that transform as $I = 2$ objects exist

$$O_1 = \bar{N}\mathcal{Q}_L N \bar{N}\mathcal{Q}_L N - \frac{\mathrm{Tr}[\mathcal{Q}^2_L]}{6}\bar{N}\boldsymbol{\tau}N \cdot \bar{N}\boldsymbol{\tau}N + \{L \leftrightarrow R\},$$

$$O_2 = 2\left(\bar{N}\mathcal{Q}_L N \bar{N}\mathcal{Q}_R N - \frac{\mathrm{Tr}[\mathcal{Q}_L \mathcal{Q}_R]}{6}\bar{N}\boldsymbol{\tau}N \cdot \bar{N}\boldsymbol{\tau}N\right), \quad (16)$$

where $\mathcal{Q}_L = u^\dagger Q_L u$, $\mathcal{Q}_R = u Q_R u^\dagger$, $u = \exp(i\boldsymbol{\tau}\cdot\boldsymbol{\pi}/(2F_\pi))$, and $Q_{L,R}$ are "spurions" transforming under the chiral group as $Q_L \to L Q_L L^\dagger$, $Q_R \to R Q_R R^\dagger$. In the electromagnetic case, $Q_L = Q_R = \tau_3/2$, while in $0\nu\beta\beta$ $Q_L = \tau^+$, $Q_R = 0$. In our conventions, O_1 enters the $\Delta L = 2$ Lagrangian with coefficient $2G^2_F V^2_{ud} m_{\beta\beta} g^{\mathrm{NN}}_\nu$. Defining the electromagnetic LECs multiplying $O_{1,2}$ as $e^2 C_{1,2}/4$, chiral symmetry dictates $g^{\mathrm{NN}}_\nu = C_1$.

In the electromagnetic case, O_1 and O_2 only differ at the multipion level, and an isospin-breaking two-nucleon observable, such as the $I = 2$ combination of scattering lengths $a_{\mathrm{CIB}} = (a_{nn} + a_{pp})/2 - a_{np}$, only constrains the sum $C_1 + C_2$. Extracting this combination from data

provides a rough estimate of g^{NN}_ν under the assumption $C_1 \sim C_2$. As in the $\Delta L = 2$ case, we introduce the dimensionless couplings $\tilde{C}_i \equiv [4\pi/(m_N\tilde{C})]^2 C_i$ and compute the scattering lengths $a_{pp,nn,np}$ including the leading sources of isospin breaking—the Coulomb potential and pion mass splitting—and $\tilde{C}_1 + \tilde{C}_2$. Similar to the $\Delta L = 2$ case, we find that $\tilde{C}_1 + \tilde{C}_2$ needs to be promoted to LO and obeys the RGE

$$\mu \frac{d}{d\mu}\frac{\tilde{C}_1 + \tilde{C}_2}{2} = \frac{1}{2}\left(1 + g^2_A \frac{m^2_{\pi^+} - m^2_{\pi^0}}{e^2 F^2_\pi}\right), \quad (17)$$

while, of course, $\tilde{C}_1$ has the same RGE as $\tilde{g}^{\mathrm{NN}}_\nu$. By fitting to a_{CIB} using $a_{np} = -23.7$ fm, $a_{nn} = -18.9$ fm, and $a_{pp} = -7.8$ fm, we find $(\tilde{C}_1 + \tilde{C}_2)/2 \approx 2.5$ at $\mu = m_\pi$ in the $\overline{\mathrm{MS}}$ scheme. Using instead the R_S scheme, we find $(\tilde{C}_1 + \tilde{C}_2)/2 \approx 2.0$ at $R_S = 0.5$ fm. This estimate, based on data and chiral symmetry, again confirms that $g^{\mathrm{NN}}_\nu \sim \mathcal{O}(F^{-2}_\pi)$. Our result is consistent with analyses based on chiral [46–49] and phenomenological potentials such as AV18 [50], which also find that, except at very low energies, long- and short-range components of the CIB interaction induce effects of similar size.

Numerical impact.—To roughly estimate the impact of the contact term, we assume for concreteness $C_1 = C_2$ and hence $g^{\mathrm{NN}}_\nu = (C_1 + C_2)/2$ at some $\bar{R}_S$ or $\bar{\mu}^{-1}$ in the range 0.002–0.8 fm. The total two-nucleon amplitude $\mathcal{A}_{\Delta L=2} = \mathcal{A}^{(\nu)}_{\Delta L=2} + \mathcal{A}^{(\mathrm{NN})}_{\Delta L=2}$ then becomes independent of the regulator, as illustrated in Fig. 2, where the widths of the horizontal bands reflect the ambiguity in the choice of the point $\bar{R}_S$ or $\bar{\mu}$ where $C_1 = C_2$ is assumed. (They do not account for the uncontrolled error of the assumption itself.) The relative size of the two components depends on R_S, with $\mathcal{A}^{(\mathrm{NN})}_{\Delta L=2}/\mathcal{A}^{(\nu)}_{\Delta L=2} \sim 30\%$ at $R_S \sim 0.1$ fm, decreasing to $\sim 10\%$ at $R_S \sim 0.6$ fm. More insight can be obtained from the matrix-element densities ρ_ν and ρ_{NN}, implicitly defined from Eqs. (14) and (15) by

$$\mathcal{A}^{(\nu)}_{\Delta L=2} = \int dr \rho_\nu(r), \qquad \mathcal{A}^{(\mathrm{NN})}_{\Delta L=2} = \int dr \rho_{\mathrm{NN}}(r). \quad (18)$$

Figure 3 (top panel) shows that $\rho_{\mathrm{NN}}(r)$ is concentrated at smaller distances than $\rho_\nu(r)$, and its contribution to the amplitude is thus partially diluted.

We have performed a similar analysis for $A = 6, 12$ nuclei, using variational Monte Carlo nuclear wave functions [51] based on the AV18 two-nucleon [50] and IL7 three-nucleon [52] interactions. The mismatch between the short-range behaviors of existing strong-interaction potentials and our $0\nu\beta\beta$ interaction introduces additional model dependence, which we mitigate by (i) considering an alternative extraction of $(C_1 + C_2)/2$ from the phase-shift analysis of Refs. [47,48], which employs the same
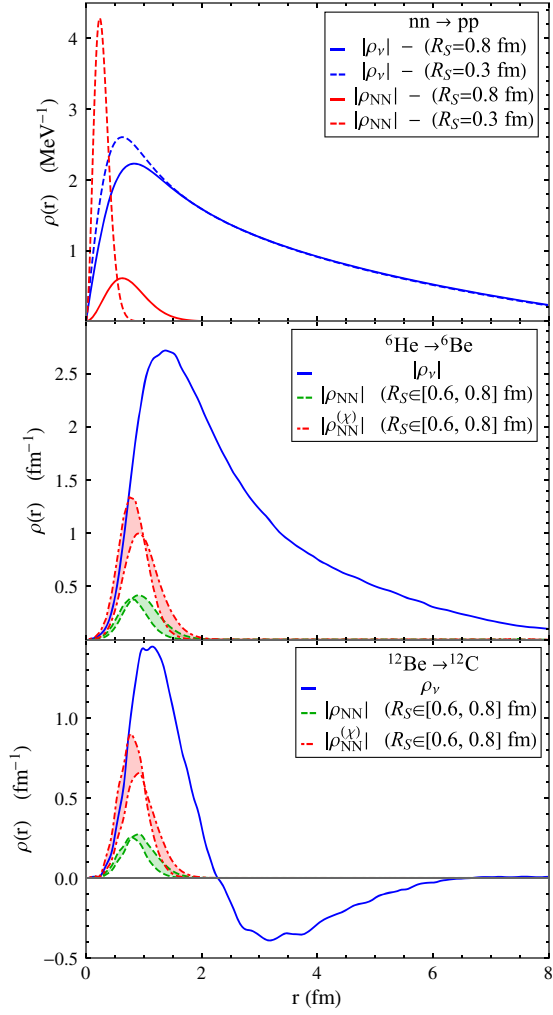
FIG. 3. $\rho_\nu(r)$ and $\rho_{NN}(r)$ for the $nn \to ppee$ process (top) and for nuclear transitions with $A = 6$ (middle) and $A = 12$ (bottom). In the middle and bottom panels, the green (ρ_{NN}) and red ($\rho_{NN}^{(\chi)}$) bands correspond to $g_\nu^{NN} = (C_1 + C_2)/2$ extracted from our analysis and from Refs. [47,48], respectively.

regulator (13) with $R_S \simeq 0.6$–0.8 fm, approximately the range of AV18's short-range part, and (ii) simply replacing our $V_{\nu,CT}(\mathbf{r})$ with AV18's short-range CIB potential. Note that $C_1 + C_2$ is related to the CIB coefficient C_0^{IT} of Refs. [47,48] by $(C_1 + C_2)/2 = -6C_0^{IT}/e^2$.

For $\Delta I = 0$ transitions such as the ^{6}He $\to ^6$Be shown in Fig. 3 (middle panel), we find $\mathcal{A}_{\Delta L=2}^{(NN)}/\mathcal{A}_{\Delta L=2}^{(\nu)} \sim 10\%$, similar to the $nn \to ppee$ case. In realistic $0\nu\beta\beta$ transitions, however, the total nuclear isospin changes by two units, $\Delta I = 2$. This implies the presence of a node in $\rho_\nu(r)$ due to the orthogonality of the initial and final spatial wave functions. The resulting partial cancellation between the regions with $r \lesssim 2$ fm and $r \gtrsim 2$ fm [51] leads to a relative enhancement of the short-range contribution, as illustrated in Fig. 3 (bottom panel) for ^{12}Be $\to ^{12}$C. Numerically, we find $\mathcal{A}_{\Delta L=2}^{(NN)}/\mathcal{A}_{\Delta L=2}^{(\nu)} \sim 25\%$ (our fit),

$\sim 55\%$ (fit from Refs. [47,48]), and $\sim 60\%$ (AV18 representation of the short-range CIB potential). Because (i) the node in the density is a robust feature of $\Delta I = 2$ transition [53,54], and (ii) the relative size of the matrix elements of short- and long-range operators is roughly the same in nuclei from $A = 10$ through $A = 136$ [51], we expect the effects in ^{12}Be $\to ^{12}$C and experimentally relevant transitions to be of comparable size.

Conclusion.—The above arguments suggest that the new leading-order short-range $\Delta L = 2$ potential identified in this Letter can affect the $0\nu\beta\beta$ amplitude and, consequently, the quantitative implications of experiments on $m_{\beta\beta}$ at the $\mathcal{O}(1)$ level. (At subleading orders, a similar analysis of the renormalization of the $0\nu\beta\beta$ amplitude must be performed, which takes into account the required modifications to Weinberg's power counting in the strong-interaction sector, such as the perturbative correction induced by the $^1S_0$ effective range at next-to-leading order [37].) In particular, sensitivity to the inverted hierarchy [24] in next-generation experiments might be increased or much decreased, depending on the size and sign of the interference between the new short-range contribution and the long-range term. We hope this will stimulate work towards a more controlled determination of g_ν^{NN} from lattice QCD and an assessment of the impact of the short-range potential in nuclei of experimental interest.

[1] J. Schechter and J. W. F. Valle, Phys. Rev. D **25**, 2951 (1982).

[2] P. Minkowski, Phys. Lett. **67B**, 421 (1977).

[3] R. N. Mohapatra and G. Senjanovic, Phys. Rev. Lett. **44**, 912 (1980).

[4] M. Gell-Mann, P. Ramond, and R. Slansky, in *Supergravity Workshop Stony Brook, New York, September 27–28, 1979, Conference Proceedings*, Vol. C790927 (1979), p. 315.

[5] S. Davidson, E. Nardi, and Y. Nir, Phys. Rep. **466**, 105 (2008).

[6] A. Gando *et al.* (KamLAND-Zen Collaboration), Phys. Rev. Lett. **110**, 062502 (2013).

[7] M. Agostini *et al.* (GERDA Collaboration), Phys. Rev. Lett. **111**, 122503 (2013).

[8] J. B. Albert *et al.* (EXO-200 Collaboration), Nature (London) **510**, 229 (2014).

[9] S. Andringa *et al.* (SNO+ Collaboration), Adv. High Energy Phys. **2016**, 1 (2016).

[10] A. Gando *et al.* (KamLAND-Zen Collaboration), Phys. Rev. Lett. **117**, 082503 (2016); **117**, 109903(E) (2016).

[11] S. R. Elliott *et al.*, arXiv:1610.01210.

[12] M. Agostini *et al.*, Nature (London) **544**, 47 (2017).

[13] J. B. Albert *et al.* (EXO Collaboration), Phys. Rev. Lett. **120**, 072701 (2018).

[14] C. Alduino *et al.* (CUORE Collaboration), Phys. Rev. Lett. **120**, 132501 (2018).

[15] O. Azzolini *et al.* (CUPID-0 Collaboration), arXiv: 1802.07791.

[16] S. Weinberg, Phys. Rev. Lett. **43**, 1566 (1979).

[17] K. S. Babu and C. N. Leung, Nucl. Phys. **B619**, 667 (2001).

[18] G. Prezeau, M. Ramsey-Musolf, and P. Vogel, Phys. Rev. D **68**, 034016 (2003).

[19] A. de Gouvêa and J. Jenkins, Phys. Rev. D **77**, 013008 (2008).

[20] L. Lehman, Phys. Rev. D **90**, 125023 (2014).

[21] M. L. Graesser, J. High Energy Phys. 08 (2017) 099.

[22] V. Cirigliano, W. Dekens, J. de Vries, M. L. Graesser, and E. Mereghetti, J. High Energy Phys. 12 (2017) 082.

[23] S. M. Bilenky and S. T. Petcov, Rev. Mod. Phys. **59**, 671 (1987); **60**, 575(E) (1988).

[24] S. M. Bilenky and C. Giunti, Int. J. Mod. Phys. A **30**, 1530001 (2015).

[25] J. Engel and J. Menéndez, Rep. Prog. Phys. **80**, 046301 (2017).

[26] V. Cirigliano, W. Dekens, E. Mereghetti, and A. Walker-Loud, arXiv:1710.01729.

[27] P. F. Bedaque and U. van Kolck, Annu. Rev. Nucl. Part. Sci. **52**, 339 (2002).

[28] E. Epelbaum, H.-W. Hammer, and U.-G. Meißner, Rev. Mod. Phys. **81**, 1773 (2009).

[29] R. Machleidt and D. R. Entem, Phys. Rep. **503**, 1 (2011).

[30] S. Weinberg, Phys. Lett. B **251**, 288 (1990).

[31] S. Weinberg, Nucl. Phys. **B363**, 3 (1991).

[32] N. Cabibbo, Phys. Rev. Lett. **10**, 531 (1963).

[33] M. Kobayashi and T. Maskawa, Prog. Theor. Phys. **49**, 652 (1973).

[34] D. B. Kaplan, M. J. Savage, and M. B. Wise, Nucl. Phys. **B478**, 629 (1996).

[35] S. R. Beane, P. F. Bedaque, M. J. Savage, and U. van Kolck, Nucl. Phys. **A700**, 377 (2002).

[36] A. Nogga, R. G. E. Timmermans, and U. van Kolck, Phys. Rev. C **72**, 054006 (2005).

[37] B. Long and C.-J. Yang, Phys. Rev. C **86**, 024001 (2012).

[38] M. Pavón Valderrama and D. R. Phillips, Phys. Rev. Lett. **114**, 082502 (2015).

[39] D. B. Kaplan, M. J. Savage, and M. B. Wise, Nucl. Phys. **B534**, 329 (1998).

[40] V. Cirigliano, W. Dekens, J. de Vries, M. L. Graesser, E. Mereghetti, S. Pastore, and U. van Kolck (to be published).

[41] N. Barnea, L. Contessi, D. Gazit, F. Pederiva, and U. van Kolck, Phys. Rev. Lett. **114**, 052501 (2015).

[42] A. Nicholson, E. Berkowitz, C. C. Chang, M. A. Clark, B. Joo, T. Kurth, E. Rinaldi, B. Tiburzi, P. Vranas, and A. Walker-Loud, Proc. Sci., LATTICE2016 (**2016**) 017.

[43] P. E. Shanahan, B. C. Tiburzi, M. L. Wagman, F. Winter, E. Chang, Z. Davoudi, W. Detmold, K. Orginos, and M. J. Savage, Phys. Rev. Lett. **119**, 062003 (2017).

[44] B. Moussallam, Nucl. Phys. **B504**, 381 (1997).

[45] B. Ananthanarayan and B. Moussallam, J. High Energy Phys. 06 (2004) 047.

[46] M. Walzl, U.-G. Meißner, and E. Epelbaum, Nucl. Phys. **A693**, 663 (2001).

[47] M. Piarulli, L. Girlanda, R. Schiavilla, R. Navarro Pérez, J. E. Amaro, and E. Ruiz Arriola, Phys. Rev. C **91**, 024003 (2015).

[48] M. Piarulli, L. Girlanda, R. Schiavilla, A. Kievsky, A. Lovato, L. E. Marcucci, S. C. Pieper, M. Viviani, and R. B. Wiringa, Phys. Rev. C **94**, 054007 (2016).

[49] P. Reinert, H. Krebs, and E. Epelbaum, arXiv:1711.08821.

[50] R. B. Wiringa, V. G. J. Stoks, and R. Schiavilla, Phys. Rev. C **51**, 38 (1995).

[51] S. Pastore, J. Carlson, V. Cirigliano, W. Dekens, E. Mereghetti, and R. B. Wiringa, Phys. Rev. C **97**, 014606 (2018).

[52] S. C. Pieper, AIP Conf. Proc. **1011**, 143 (2008).

[53] F. Šimkovic, A. Faessler, V. Rodin, P. Vogel, and J. Engel, Phys. Rev. C **77**, 045503 (2008).

[54] J. Menéndez, A. Poves, E. Caurier, and F. Nowacki, Nucl. Phys. **A818**, 139 (2009).